Supplement of Nat. Hazards Earth Syst. Sci., 25, 1769–1788, 2025
https://doi.org/10.5194/nhess-25-1769-2025-supplement

Natural Hazards and Earth System Sciences
Open Access

Supplement of

An appraisal of the value of simulated weather data for quantifying coastal flood hazard in the Netherlands

Cees de Valk and Henk van den Brink

Correspondence to: Cees de Valk (cees.de.valk@knmi.nl)

Please note that references to numbered sections, figures, tables and equations without "S" refer to the main text.

S1 Uncertainty of return value estimates from measurements

As an illustration of the uncertainty of return value estimates from measurement data, Fig. S1 shows estimates of return values of water level at Hoek van Holland (tidal station 2 in Fig. 1) derived from the 1% highest trend-corrected high water values measured since 1887 (black curve) with their 95% confidence intervals (vertical bars). The top panels show estimates using a Generalized Pareto (GP) tail and the bottom panels show estimates using Generalized Weibull (GW) tail. The methods are as described in Sect. 4 with one exception: the estimated return values are considered to be log-normally distributed rather than normally distributed, as this produces more plausible intervals in the case of very high uncertainty (in the limit, both are valid approximations).

For the longest return periods, the confidence intervals are very wide: about 2 m for a return period of 10,000 years and 6 m for a return period of 10^7 years for the GP tail. In fact, the estimates in the landmark study Dillingh et al (1993) have even wider confidence intervals. Also shown in Fig. S1 (left) are the estimates from the measurements up to 1955 (blue) and after 1955 (red) along with the corresponding data points. These estimates are very different, spanning almost the entire widths of the confidence intervals of the estimates from the complete dataset. Further, splitting the data of odd and even years (Jul to Jun), similarly large differences are found; see Fig. S1 (right). This underscores that the large uncertainty implied by these confidence intervals is realistic.

In fact, high uncertainty of return value estimates makes it impossible to properly account for this uncertainty in the flood risk analysis (e.g. Ditlevsen and Madsen, 1996, Sect. 3.4): in order to account for uncertainty, the uncertainty should be reliably quantified, but that need not be the case. For example, in Fig. S1 (left), the estimates from the complete dataset (presumably the most reliable) lie far outside the confidence intervals derived from the data after 1955. If only the latter were available, the uncertainty would be seriously underestimated. This is a fundamental problem, not related to the method used to estimate the uncertainty: the uncertainty of an estimate generally depends on the true value (e.g. de Haan and Ferreira, 2006, Sect. 3.4.2), but the true value is not known.

For estimates based on the GW tail Fig. S1 (bottom), the confidence intervals are clearly less wide than for estimates based on the GP tail (top). However, the uncertainties are still of similar order of magnitude, so using a GW tail for estimating return periods would not solve the problems signaled above.

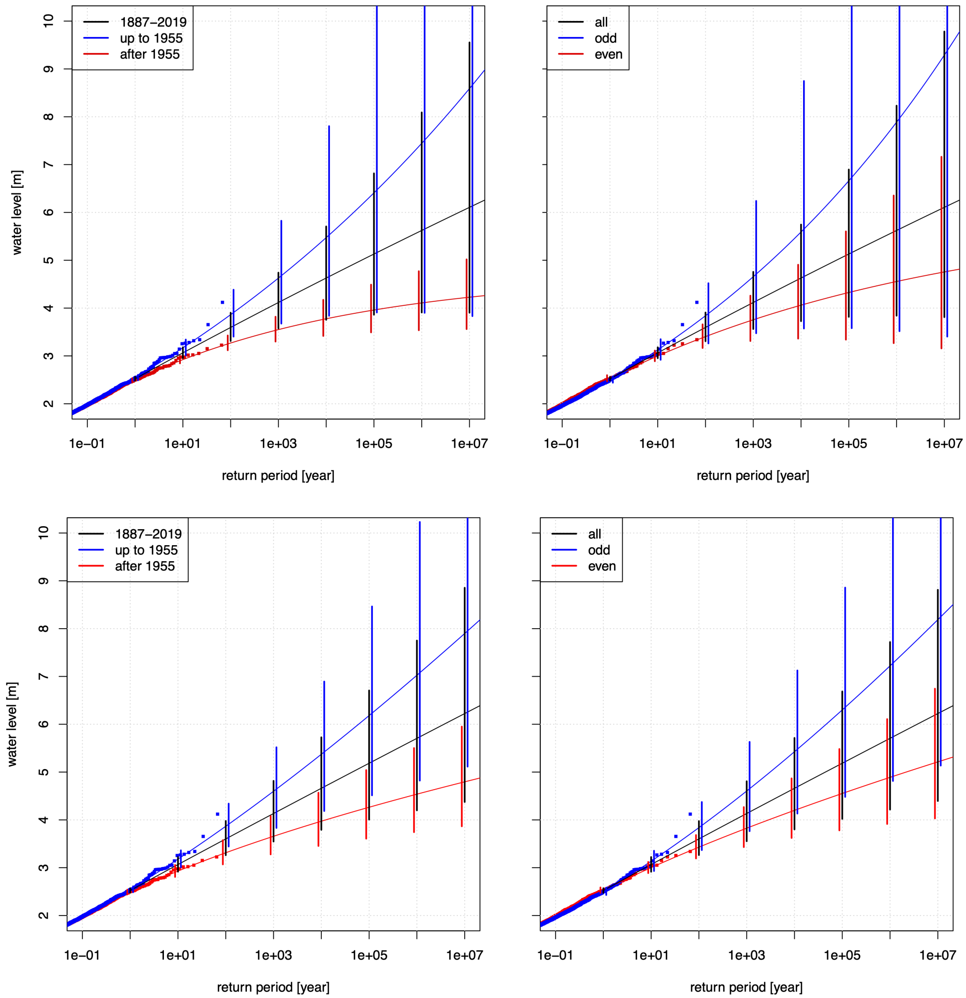

Figure S1. Estimates of return values of sea level at Hoek van Holland from trend-corrected measurement data (black curve) with 95% confidence intervals (thick black lines). Left: data and estimates from measurements made up to (blue) and after (red) 1955. Right: data and estimates from even (red) and odd (blue) years. Top: Generalized Pareto (GP) tail; bottom: Generalized Weibull (GW) tail.

S2 Tail dependence of stress from different ensemble members

To check for dependence between the extremes from two time-series, a sensitive metric is the coefficient of tail dependence η from (Ledford and Tawn, 1996, 1997, 1998); see Subsection 7.4. We consider estimates of $\rho := 2\eta - 1$, which can be interpreted similarly as an ordinary Pearson correlation coefficient for two Gaussian random variables (although it is estimated in a very different way!). In particular, 0 means that conditional on one of the two variables exceeding a high threshold, they are effectively independent.

To check the dependence between extremes of stress from different ensemble members of the SEAS5 forecast data for ranges in excess of one month used in de present study, we estimated ρ from all pairs of simultaneous values from different ensemble members. Estimates are made from different fractions p of the "most extreme" pairs. Because the estimates may be biased by seasonality in the data, we made estimates from all data, but also for the long storm season ONDJFM and a shorter season DJF; see Fig. S2.

For both the long and the short storm season, the tail correlation coefficient tends to practically 0 for small sample fractions, showing that the dependence between extremes of stress from different members is negligible. This supports the treatment of data from different SEAS5 ensemble members as independent in the statistical analysis.

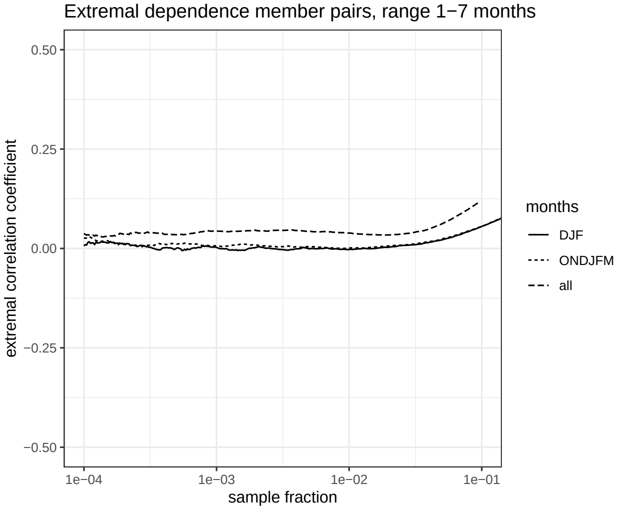

Figure S2. Estimates of tail correlation coefficient $\rho := 2\eta - 1$ from all pairs of ensemble members of SEAS5 forecasts of stress for ranges exceeding 1 month from grid point b (see Fig. 2) for months DJF (drawn), ONDJFM (dotted) and all year (dashed), derived from different sample fractions.

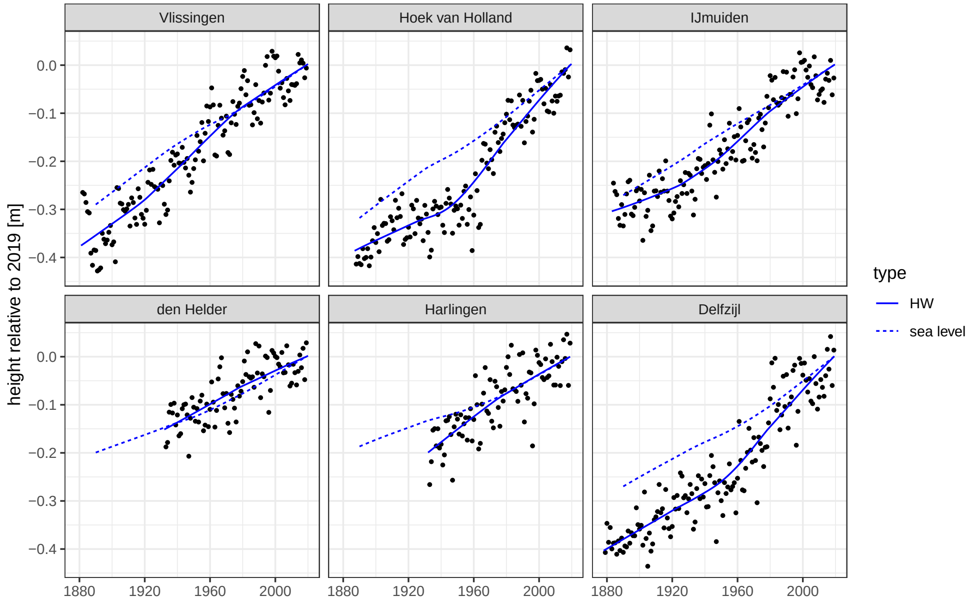

Figure S3. Time-series of annual mean HW (dots) with trend line (full) relative to the trend line value in 2019, and trend line of annual mean sea level relative to its value in 2019 (dashed).

S3 Detrending of HW measurements

Figure S3 shows the annual mean HW and its trend line relative to the trend value in 2019 (estimated using a loess filter with span equal to $84/n$ with n the record length) for the six tidal stations. Additionally, the estimated trend line for the annual mean sea level (relative to its value in 2019) is plotted. The trends are increasing and, except for Den Helder, larger than the sea level rise. The plots for most stations show an accelerated rise in annual mean HW between roughly 1940 and 1980 which is not seen in the sea level rise. These deviations are largely attributed to hydraulic engineering interventions (Dillingh, 2013) but natural processes may also play a role. The records of HW were de-trended assuming that a change in the average HW has the same effect on the extreme HW values.

The considerable differences between the trends of annual mean HW and of annual mean sea level observed in Fig. S3 indicate that extrapolated trends of annual mean sea level may not be suitable for normalizing reconstructed peak values of HW or skew surge of historical flood events as in (Van Gelder, 1996; Baart, 2011). Using these reconstructions in the estimation of return levels to increase the accuracy (see Sect. 2) may bias the estimates.

To check the de-trending of the measured HW, several checks have been performed on the time evolution of the more extreme HWs after the correction: the annual 99% quantiles and the annual maxima; see Fig. S4. Clear residual trends cannot be discerned in these; apparent deviations are limited to short periods at the beginning or end of a record, where the trend estimation may be less accurate.

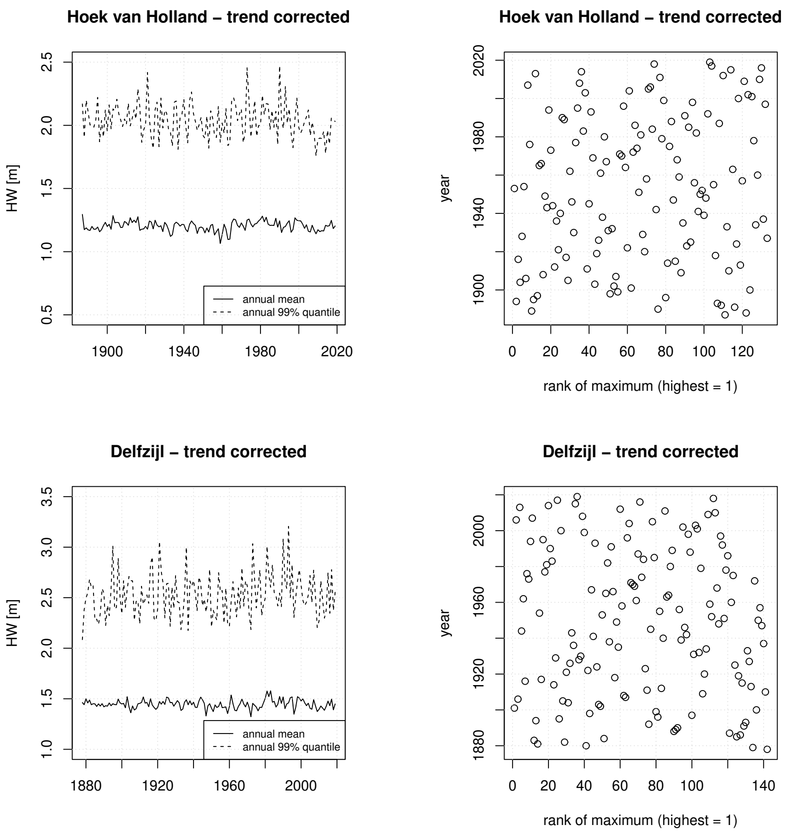

Figure S4. Annual means and 99% quantiles of trend-corrected HW (left), and year as function of the rank of the annual maximum of HW (highest = 1) (right) for Hoek van Holland (top) and Delfzijl (bottom).

In the 99% quantiles, a very small fluctuation can be observed with a minimum around 1960 and maximum around 1920 and 1990, which resembles the pattern of the winter North Atlantic Oscillation (NAO). However, this is of little practical relevance.

S4 Saturation of the drag coefficient

Measurements in the laboratory and at sea (e.g. Curcic (2020); Richter et al (2021) and their references) indicate that the drag coefficient over sea saturates to a value of about 0.003 for wind speeds in the range of 25-35 m s^{-1}. Various empirical and physics-based models have been proposed, but the issue is far from settled. In fact, the ECMWS IFS model, which employs a dynamic wind-wave coupling to compute stress and near-surface wind speed, exhibits saturation even though this is not explicitly incorporated in the model (Pineau-Guillou et al, 2018). This is also seen in the SEAS5 data (generated using the IFS model); see Fig. S5 for an example (this drag relation from SEAS5 should not be trusted quantitatively, because empirical return values of wind speed from SEAS5 along the Dutch coast are considerably lower than those from wind measurements at nearby stations (not shown)). Both measurements (Fig. 3 of Curcic (2020)) and these simulated data suggest that drag saturation, if real, should be rather smooth, hence would not lead to an anomaly in the tail distribution of stress and/or near-surface wind speed. Furthermore, if drag saturation would not affect the geostrophic wind, then it would affect near-surface wind speed more than it affects stress, as can be assessed using the simple expression of Blackadar and Tennekes (1968) of wind and stress in a neutrally stable boundary layer as functions of the geostrophic wind; see also Zweers et al (2012). Finally, two-way interaction between stress and cyclone strength (Sect. 5.3) may further reduce the influence of drag saturation on the tail of stress.

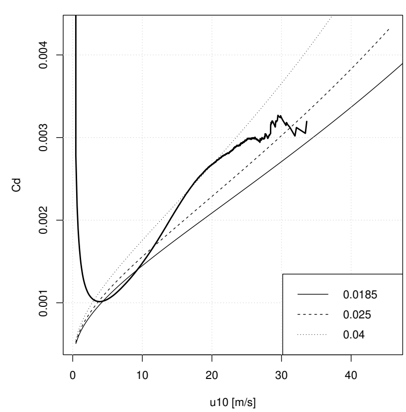

Figure S5. Empirical drag coefficient C_d from SEAS5 data for grid point b in Fig. 2 (thick). The thin lines are determined from Charnock relations with various constants (see legend)

S5 Return value estimates for stress

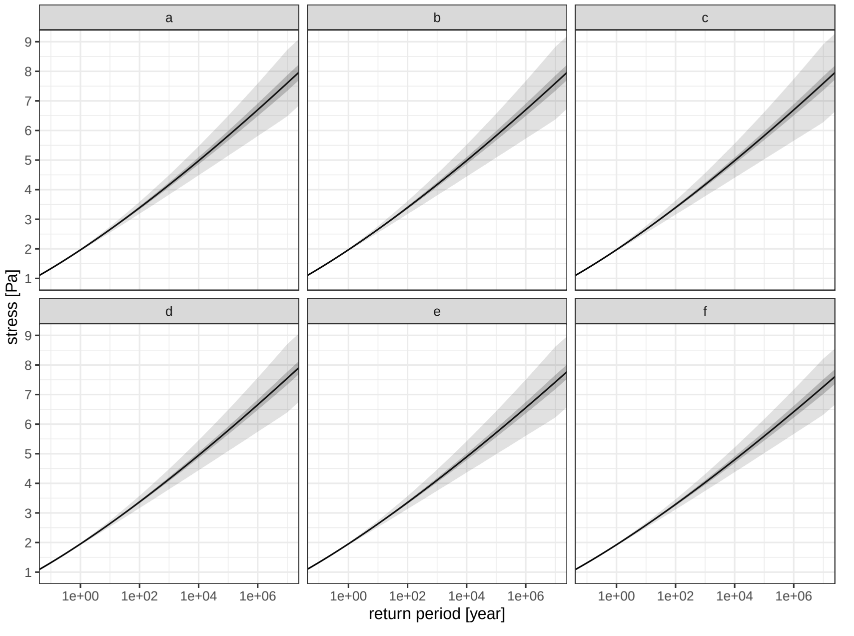

Figure S6. Return value estimates for stress derived from the corrected SEAS5 stress data with sampling error (95% confidence intervals; dark gray) and assessment of total uncertainty (idem, light gray). Grid point labels in headers refer to the triangles in Fig. 2.

S6 Generalized Weibull tail estimation

For fitting Generalized Weibull (GW) tails, we employ an adaptation of the estimator from de Valk and Cai (2018). The latter is introduced there as an estimator for the log-GW tail de Valk (2016a); to estimate the GW tail from a data sample, one simply skips the step of taking logarithms of the data values.

In de Valk and Cai (2018), the large-sample behaviour of this estimator was analysed in a configuration using different thresholds for shape and scale estimation. In practice, however, it proves to be more effective to use the same thresholds; see also Albert et al (2015). A slight modification of the asymptotic analysis in de Valk and Cai (2018) shows that with that approach, errors in return value estimates are dominated by the error in the shape estimate.

Furthermore, in the notation of de Valk and Cai (2018), the estimator $\hat{\theta}_{k_n,n}$ of the shape parameter θ in their Eq. (19) is modified by replacing $\hat{\gamma}^H_{i,n}$ with the asymptotically equivalent expression

$$\left(\vartheta_{i+1,n}\tfrac{1}{i}\sum_{j=1}^{i} h_{\hat{\theta}_{k_n,n}}(\vartheta_{j,n}/\vartheta_{i+1,n})\right)^{-1}\hat{\gamma}^H_{i,n}. \tag{S1}$$

This modification is motivated by replacing the first approximation of $g(\vartheta_{i+1,n})$ in Eq. (17) of de Valk and Cai (2018) with the second, more accurate, approximation. It leads to an implicit equation for the shape parameter, which can be solved approximately by searching over a discrete set of values.

The code used is the R function FitGW_iHilli.R.available at https://github.com/ceesfdevalk/EVTools.

In practice, the outcomes of this estimator resemble those of the maximum likelihood (ML) method, but the computation takes much less time. An alternative estimator is presented in Albert et al (2015).

S7 Error in skew surge predictions on the Waddenzee

For the high-resolution shallow-water surge-tide model DCSM-FM 100m (Zijl et al, 2022), the bias in the predictions of skew surge at Harlingen (5) and Delfzijl (6) is shown in Fig. S7, reproduced from Zijl and Laan (2021). The predicted skew surge has a negative bias above a threshold close to the 99% quantile; the magnitude of the bias increases approximately linearly in the excess of surge above this threshold.

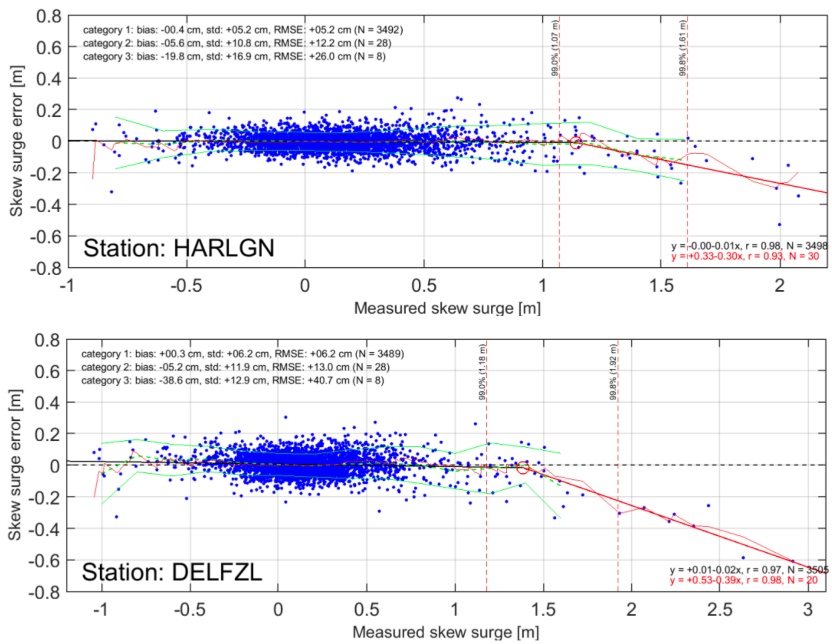

Figure S7. Error in predictions of skew surge at Harlingen (5) (top) and Delfzijl (6) (bottom) by the DCSM-FM 100m tide-surge model forced by HIRLAM output for the period 2013-2017. From Zijl and Laan (2021) (with permission).

This finding can be used to correct water level simulations by the DCSMv5 surge-tide model forced by SEAS5 stress and mslp fields (Sect. 3). For this purpose, we use the affine relations between surge predictions from DCSM-FM 100m and from DCSMv5 in Fig. 7 together with the bias in DCSM-FM 100m (red lines in Fig. S7) to correct the full datasets of skew surge from DCSMv5 forced by SEAS5 (see Sect. 3). These are subsequently combined with astronomical tide to compute bias-corrected HW.

GW-shape estimates from the original and the bias-corrected HW data for Harlingen and Delfzijl are shown in Fig. S8, complementing Fig. 7. We observe a substantial increase in shape parameter estimates at low thresholds (exceeded by high fractions of the sample). The large effect of bias correction is probably somewhat exaggerated: it is assumed that the bias in the skew surge in Fig. S7 has a kink at a certain surge level and is affine above and below this level. In reality, the bias will likely transition smoothly as a function of the skew surge. This is consistent with the shape estimates from measurement data: these fall nicely between the estimates from the bias-corrected and from the original DCSMv5 data. For thresholds above the kink, the latter two estimates are almost identical, as claimed. The chosen thresholds (at a sample fraction of 1.2%) appear to be representative for the estimates at these higher thresholds (or are slightly higher than these).

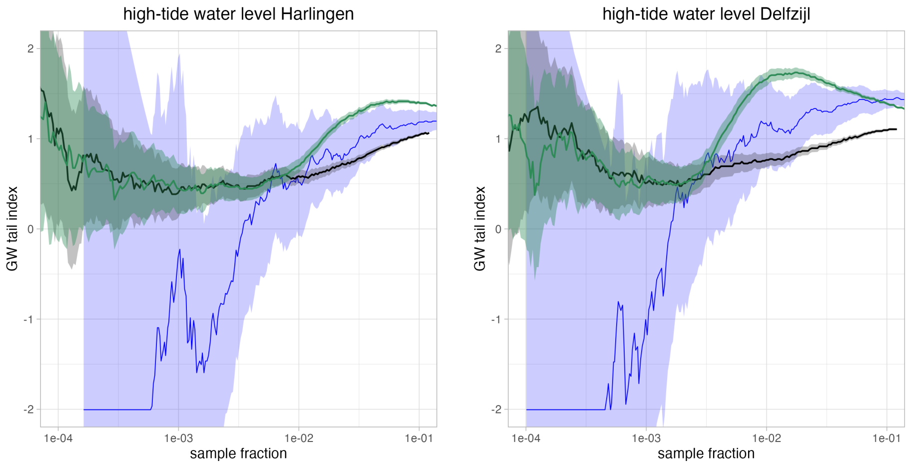

Figure S8. Estimates of the shape parameter of the GW tail of HW for Harlingen and Delfzijl from measurements (blue), simulated data from the DCSMv5 model forced by SEAS5 (black), and bias-corrected simulated data (green) with 95% confidence intervals, against the fraction of the sample used for estimation. Bias correction is based on the fitted relations displayed in Figs. S7 and 7.

References

Albert, C., Dutfoy, A., Gardes, L., Girard, S.: An extreme quantile estimator for the log-generalized Weibull-tail model. Econometrics and Statistics, 13, 137–174, 2020.

Baart, F., Bakker, M. A. J., Van Dongeren, A., Den Heijer, C., Van Heteren, S., Smit, M. W. J., ... : Using 18th century storm-surge data from the Dutch Coast to improve the confidence in flood-risk estimates. Nat. Hazards Earth Syst. Sci., 11(10), 2791–2801, 2011.

Bengtsson, L., Andrae, U., Aspelien, T., Batrak, Y., Calvo, J., de Rooy, W., Odegard Koltzow, M.: The HARMONIE-AROME model configuration in the ALADIN-HIRLAM NWP system. Mon. Weather Rev., 145, 1919–1935, 2017.

Blackadar, A. K. and Tennekes, H.: Asymptotic similarity in neutral barotropic planetary boundary layers. Journal of the Atmospheric Sciences, 25(6), 1015–1020, 1968.

van den Brink, H.W.: Het gebruik van de ECMWF seizoensverwachtingen voor het berekenen van de klimatologie van extreme waterstanden langs de Nederlandse kust. Report TR-385, KNMI, de Bilt, 2020.

Curcic, M. and Haus, B.K.: Revised estimates of ocean surface drag in strong winds. Geophysical research letters, 47(10), p.e2020GL087647, 2020.

Dillingh, D., De Haan, L., Helmers, R., Können, G.P., Van Malde, J.: De basispeilen langs de Nederlandse kust, Statistisch onderzoek, Report DGW-93.023, Rijkswaterstaat Dienst Getijdewateren, 1993.

Dillingh, D.: Veranderingen in gemiddelde zeeniveaus in de Nederlandse kustwateren. Report 1206182-000, Deltares, 2013.

Ditlevsen, O., Madsen, H. O.: Structural reliability methods. Wiley NY, 1996.

Dombry, C.: Existence and consistency of the maximum likelihood estimators for the extreme value index within the block maxima framework. Bernoulli, 21(1), 420–436, 2015.

Ferro, C. A., Segers, J.: Inference for clusters of extreme values. Journal of the Royal Statistical Society: Series B (Statistical Methodology), 6(2), 545–556, 2003.

Van Gelder, P.H.A.J.M.: A new statistical model for extreme water levels along the Dutch coast. Stochastic hydraulics, 96, 243–249, 1996.

de Haan, L., Ferreira, A.: Extreme value theory - An introduction. Springer, 2006.

Ledford, A. W., Tawn, J. A.: Statistics for near independence in multivariate extreme values. Biometrika, 83(1), 169–187, 1996.

Ledford, A. W., Tawn, J. A.: Modelling dependence within joint tail regions. Journal of the Royal Statistical Society: Series B (Statistical Methodology), 59(2), 475–499, 1997.

Ledford, A. W., Tawn, J. A.: Concomitant tail behaviour for extremes. Advances in applied Probability, 30(1), 197–215, 1998.

Pineau-Guillou, L., Ardhuin, F., Bouin, M. N., Redelsperger, J. L., Chapron, B., Bidlot, J. R., Quilfen, Y.: Strong winds in a coupled wave–atmosphere model during a North Atlantic storm event: Evaluation against observations. Quarterly Journal of the Royal Meteorological Society, 144(711), 317–332, 2018.

Richter, D.H., Wainwright, C., Stern, D.P., Bryan, G.H. and Chavas, D.: Potential low bias in high-wind drag coefficient inferred from dropsonde data in hurricanes. Journal of the Atmospheric Sciences, 78(7), 2339–2352, 2021.

de Valk, C.: Approximation of high quantiles from intermediate quantiles. Extremes, 19, 661–686, 2016a.

de Valk, C., Cai, J.J.: A high quantile estimator based on the log-Generalised Weibull tail limit. Econometrics and Statistics, 6, 107–128, 2018.

de Valk, C.F., van den Brink, H.W.: Comparison of tail models and data for extreme value analysis of high tide water levels along the Dutch coast. Report WR-23-01, KNMI, De Bilt, 2023a.

de Valk, C.F., van den Brink, H.W.: Update van de statistiek van extreme zeewaterstand en wind op basis van meetgegevens en modelsimulaties. Report TR-406, KNMI, De Bilt (in Dutch), 2023b.

Zijl, F., Laan, S.: Impact golfkoppeling DCSM-FM. Memo 11206814-004-ZKS-0008, Deltares, Delft, 2021.

Zijl, F., Zijlker, T., Laan, S., Groenenboom, J.: DCSM-FM 100m: a sixth-generation model for the NW European Shelf. Report 11208054-004-ZKS-0002, Deltares, Delft (https://publications.deltares.nl/11208054_004_0002.pdf), 2022.

Zweers, N. C., Makin, V. K., De Vries, J. W., Burgers, G.: On the influence of changes in the drag relation on surface wind speeds and storm surge forecasts. Natural hazards, 62, 207-219, 2012.